Heliyon 9 (2023) e16220

Contents lists available at ScienceDirect

Heliyon

journal homepage: www.cell.com/heliyon

Research article

Associations between preprocedural carotid artery perivascular fat density and early in-stent restenosis after carotid artery stenting

Jun Hu [a,b,1], Na Hu [c,1], Tiemin Hu [b], Jiwei Zhang [b], Dong Han [d], Hong Wang [a,*]

[a] Faculty of Integrated Traditional Chinese and Western Medicine, Hebei University of Chinese Medicine, Shijiazhuang, China
[b] Department of Neurosurgery, Affiliated Hospital of Chengde Medical University, Chengde, China
[c] Department of Radiology, Chengde Central Hospital, Chengde, China
[d] Department of Radiology, Affiliated Hospital of Chengde Medical University, Chengde, China

ARTICLE INFO

Keywords:
Carotid artery stenting
Computed tomographic angiography
Perivascular fat density
In-stent restenosis
Inflammation

ABSTRACT

Objectives: This study investigated the association between perivascular fat density (PFD) via preoperative computed tomographic angiography (CTA) and early in-stent restenosis (ISR) after carotid artery stenting (CAS).

Methods: We retrospectively evaluated 248 consecutive patients who had undergone initial CAS and received a preoperative cervical CTA examination between January 2019 and October 2020. The patients were categorized into two according to whether they sustained ISR during the 2 years postoperative follow-up period. Correlations between PFD and ISR were assessed, and multivariate regression for evaluating predictors of ISR was conducted. Receiver operating characteristic (ROC) curves were used to determine the cutoff value for the PFD.

Results: A total of 181 eligible patients (mean age 61.25 ± 10.35 years, 57 male) were enrolled. The ISR group had a higher proportion of closed-cell stents (48.8% versus 27.5%; $p = 0.009$) and a greater degree of residual stenosis (28[20,33] % versus 20[14.75,30] %; $p < 0.001$) than the non-ISR group. The ISR group had a higher mean HU value of PFD than the non-ISR group on the operated side (−42.26 ± 6.81 versus −59.66 ± 10.75; $p < 0.001$). The degree of residual stenosis (OR 1.146, 95%CI 1.071–1.226, $p < 0.001$) and PFD on the operated side (OR1.353, 95%CI 1.215–1.506, $p < 0.001$) were significantly associated with the ISR.

Conclusions: The occurrence of the early ISR after CAS is associated with a higher PFD on the operated side. The results indicate that PFD is a promising marker to predict the ISR after CAS.

1. Introduction

Carotid artery stenosis is a major cause of cerebral infarction and accounts for 7%–20% of all ischemic strokes [1]. As interventional technology evolves rapidly, carotid artery stenting (CAS) is becoming a minimally invasive, simple, and effective option to treat extracranial carotid artery stenosis [2,3]. However, early in-stent restenosis (ISR) is a common postoperative complication of CAS that boosts the risk of recurrent ischemic stroke or major vascular events, limits the benefit of interventional treatment, and poses a significant threat to patients, though the majority of carotid artery ISR patients remain asymptomatic [4,5]. Therefore, identifying

* Corresponding author. Faculty of Integrated Traditional Chinese and Western Medicine, Hebei University of Chinese Medicine, No. 326, Xinshi South Road, Qiaoxi District, Shijiazhuang, Hebei Province, China.
E-mail address: bossw@vip.sina.com (H. Wang).
[1] Jun Hu and Na Hu have contributed equally to this work.

https://doi.org/10.1016/j.heliyon.2023.e16220
Received 10 February 2023; Received in revised form 4 May 2023; Accepted 10 May 2023
Available online 25 May 2023

Abbreviations

CAS	carotid artery stenting
ISR	in-stent restenosis
PVAT	perivascular adipose tissue
CTA	computed tomography angiography
PFD	perivascular fat density
NASCET	North American Symptomatic Carotid Endarterectomy Trial
ICA	internal carotid artery
HU	Hounsfield units
ROI	regions of interest
DSA	digital subtraction angiography
BMI	body mass index
ROC	receiver operating characteristic

sensitive factors for early ISR prediction plays a vital role in continuously improving the long-term efficacy of CAS treatment.

Inflammation plays a critical role in ISR development [6]. Elevated circulating inflammatory markers, such as neutrophil-to-lymphocyte ratio and neutrophil-to-albumin ratio, can predict ISR after CAS but have limitations in their ability to represent vascular inflammation located in the context of specialized regions [7,8]. Inflammatory components are contained in perivascular adipose tissue (PVAT), which can contribute to inflammation and oxidative stress in local vascular tissues [9]. Moreover, it has been shown that the inflammatory changes in PVAT surrounding the carotid artery can be evaluated using computed tomography angiography (CTA) as areas of increased perivascular fat density (PFD) [10]. Recent studies have provided evidence that the increased PFD of the carotid artery is associated with cerebrovascular ischemic symptoms, ischemic stroke from an undetermined embolic source, and the occurrence of intraplaque hemorrhage [11–13]. A thorough search of the literature shows that there is no incontrovertible evidence to show that PFD is related to early ISR after CAS. The aim of this current study was to investigate the potential association between PFD, the severity of local inflammation measured by the attenuation in the carotid PVAT on CTA, and the presence of early ISR in carotid artery stenosis patients who had undergone initial CAS.

2. Methods

2.1. Patient recruitment

In this single-center retrospective observational study, we performed head and neck CTA screening at our institution consecutively from January 2019 to October 2020 to identify patients meeting the following inclusion criteria: (1) All patients treated with initial CAS procedure and had completed preprocedural CTA imaging within a week of admission. (2) Measurement criteria for the degree of carotid stenosis were based on the North American Symptomatic Carotid Endarterectomy Trial (NASCET), with symptomatic carotid stenosis≥50% and asymptomatic carotid stenosis≥60% [14,15]. (3) Patients who were followed up for at least 2 years with antiplatelet aggregation therapy (dual antiplatelet therapy with a combination of aspirin and clopidogrel for 1–3 months after the initial CAS, followed by lifelong monotherapy). We excluded patients with carotid artery stenosis caused by nonatherosclerotic factors

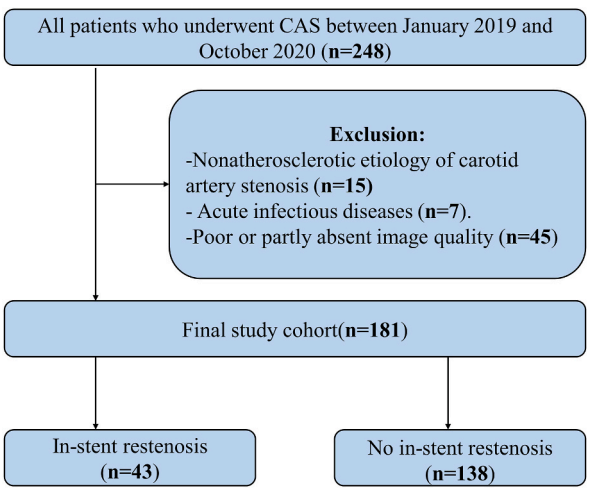

Fig. 1. Flowchart of patient enrollment.

(arteritis, dissection, radiological damage). Patients with complicated perioperative fever, acute infection of the respiratory tract, acute diarrhea, and other diseases that could cause systemic inflammatory reactions were also excluded. We also excluded patients with poor CTA images or partly absent quality images (Fig. 1).

Approval was obtained from the ethics committee of the affiliated hospital of Chengde Medical University (ethics number: LL2020011). The Declaration of Helsinki provided ethical guidelines, and a retrospective design based on routine clinical data exempted from informed consent requirements.

2.2. CTA protocol

CTA of the head and neck was performed before CAS using one of the following three CT scanners: dual-source CT (Siemens Health care, Germany), Aquilion One CT (Toshiba Medical Systems, Japan), and Revolution CT (GE Health care, USA). CTA imaging acquisition was conducted using a helical scanning mode, which covered the entire aortic arch to the vertex of the skull during the acquisition process. Iodinated contrast (Iopamidol, 370 mg iodine/ml, 50–70 ml, Hengrui Medicine Co. Ltd, China) was administered intravenously through an electric power injector at 4 ml/s. The CTA scanning was triggered by an automatic bolus-tracking system, and parameters for carotid arteries included 100–120 kV tube voltage, 1.0 pitch, 0.5–0.75 mm reconstructed slice thickness, 0.5–0.75 mm reconstructed slice interval, and 280–350 m s rotation time. The detailed scanning parameters of different CT devices are listed in Supplementary Table S1.

2.3. PFD measurement

All CTA images were transferred to the ADW4.7 workstation (GE Healthcare, Milwaukee, WI, USA) for processing. By using this dedicated workstation, we manually drew the region of interest (ROI) and measured the carotid artery perivascular fat density (PFD) value. Hounsfield units (HU) are used to measure the value of PFD surrounding the extracranial ICA. Adipose tissue pixels were identified with predefined CTA image display settings according to a previously described procedure [11]. The axial slice of carotid artery on the operated side with the maximal stenosis was selected for analysis. Two separated regions of interest (ROI) were assigned to the perivascular fat tissue surrounding the operated side and the same axial contralateral side of the ICAs (Fig. 2). Sites of maximal stenosis and fat pads encircling carotid arteries determined the location of the ROI. Mean HU values were obtained from the ROI. Each ROI measured 2.5 mm^2 in diameter and was plotted a minimum of 1 mm away from the carotid artery's outer margin, including detectable fat density (confirmed by the range of −190 HU to −30 HU) without interference from the carotid wall or surrounding structures [16]. Two radiologists who were blinded to clinical data and the degree of restenosis after CAS (N.H. and D.H. with 9 and 6 years of experience, respectively, in cerebrovascular imaging) measured the mean values of PFD (mean HU) from the two ROIs, and the averaged values of the two ROIs were used for subsequent analyses. Disagreements between the observers were resolved through consensus.

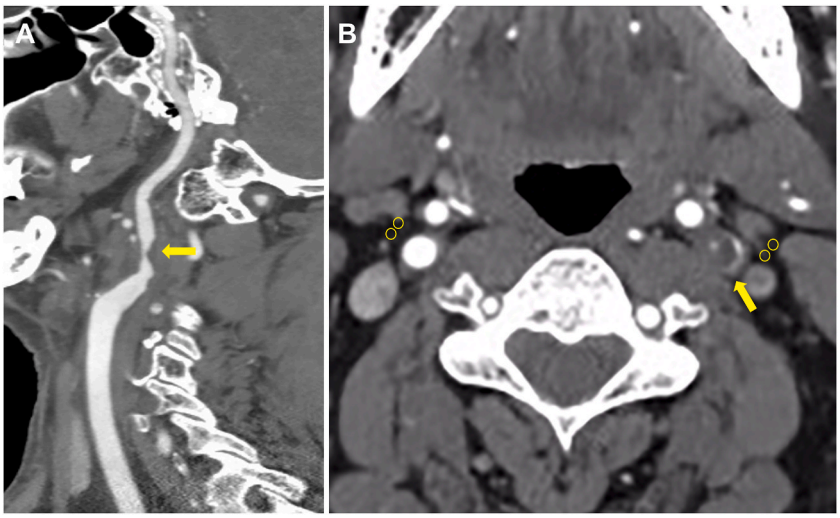

Fig. 2. Preoperative carotid CTA image to measure PFD. A: Sagittal view showing the site of maximal stenosis of the proximal internal carotid artery (yellow arrow). B: Axial view showing two ROIs (yellow circles), placed in the perivascular fat for measured PFD. In this case, the two left ROIs were −42.8HU and −43.2HU, and the two right ROIs were −72.8HU and −63.8HU. (For interpretation of the references to colour in this figure legend, the reader is referred to the Web version of this article.)

2.4. CAS procedure and stent features

CAS was performed using DSA under local anesthesia and patients received oral dual antiplatelet therapy for at least 3 days before the procedure. Weight-adjusted heparin (70 IU/kg) was intravenous infusions continuously after the groin puncture was successfully implanted into the femoral artery sheath. A distal embolic protective device was released across the lesion of the stenosis to prevent cerebral embolisms caused by shattered plaques after the 6 F or 8 F guiding catheter was located in the vicinity of the stenosis. After that, a self-expandable and suitable size stent, including open-cell stent Protégé (Medtronic, USA), Precise (Cordis, USA), or Acculink (Abbott Vascular, USA), and closed-cell stent wallstent (Boston Scientific, USA), was released and planted in the appropriate stenosis position. An angiography was performed immediately after stenting to assess any residual stenosis based on NASCET criteria. Some patients with severe stenosis required predilation. An additional postdilation procedure was typically performed in patients with residual stenosis of at least 50%. Data on stent features, including predilation and postdilation rate, stent design, and the degree of residual stenosis, were collected.

2.5. Radiological follow-up and the early ISR definition

In all patients after stenting, radiographic examinations, including CTA, digital subtraction angiography (DSA) or duplex ultrasound, were performed at 3 months, 6 months, and yearly for follow-up. Additional radiographic evaluation was also performed in patients who suffered recurrent neurological symptoms in the follow-up period. The early ISR was defined as $\geq$50% of the luminal stenosis occurring at the entire length of the stent or within 3 mm of the stent edge during the follow-up of 2 years after the CAS procedure [17,18] (Fig. 3).

2.6. Baseline assessment

A baseline demographic profile including age, sex, and body mass index (BMI) was obtained from our single-center prospective database. Each patient's vascular risk factors were also collected, including their hypertension history (blood pressure >140/90 mmHg on admission or previous medical records) [11], and diabetes mellitus (hemoglobin A1c (HbA1c) $\geq$ 6.5% or on diabetic medications). Vascular risk factors also include dyslipidemia (serum triglycerides >1.7 mmol/L, low-density lipoprotein >3.4 mmol/L, high-density lipoprotein cholesterol <0.8 mmol/L, or on statins) [19], current smoking (smoking $\geq$1 cigarette per day for more than 6 months continuously), and coronary artery disease (history of the previous diagnosis).

2.7. Statistical methods

The sample size calculation was performed with the Tests for One ROC Curve module in PASS 11 software (NCSS, LLC, Kaysville, UT, USA). Previous studies have reported that the area under the receiver operating characteristic curve (AUC) of other imaging or blood biomarkers to predict carotid restenosis was 0.737–0.935 [20–22], so we assumed that a minimum AUC of 0.7 was required for

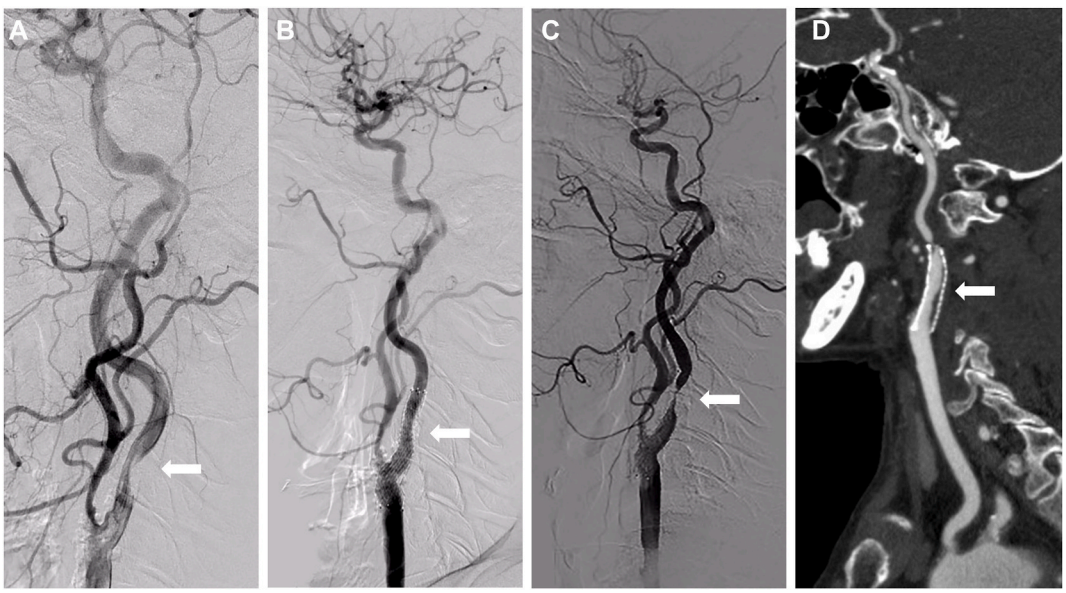

Fig. 3. ISR of the left carotid artery was detected in a 67-year-old male patient via CTA and DSA. A: Presenting DSA. B: Poststenting DSA. C, D: In-stent restenosis was observed in follow-up DSA and CTA 21 months after the stenting, respectively, (white arrow showing the stenosis section of the carotid artery).

the carotid PFD. With a power (1 -β) of 0.9 and α = 0.05, ISR-positive group: ISR-negative group = 1:3, it was calculated that at least 172 patients (43 in the ISR-positive group and 129 in the ISR-negative group) were required. To allow for about a 5% dropout rate, 181 patients were finally recruited for this study.

The intraclass correlation coefficient was used to measure the agreement between the two neuroradiologists. Kruskal–Wallis test was used to analyze mean HU differences across CT devices. Numerical variables were tested for normality using the Kolmogorov–Smirnov test. The normally distributed data were described as the mean ± standard deviation (SD) and compared by the two-sample independent *t*-test between groups. The median (P25 and P75) was used to present non-normal distribution data, and the Mann–Whitney *U* test was applied to compare differences between groups. The categorical variables were presented as frequencies and percentages (%). Differences in categorical variables were analyzed using Chi-square or Fisher's exact test. Multivariable logistic regression was used to evaluate the independent predictors of ISR. In univariate analysis, variables with $p < 0.05$ were entered into the multivariate logistic regression model. An analysis of receiver operating characteristic (ROC) curve was used to evaluate the ability of PFD to predict ISR. Statistical significance was determined by two-tailed tests with a $p < 0.05$. IBM SPSS Statistics software, version 26.0 (IBM Corporation, Armonk, New York, USA), was used for all statistical analyses.

3. Results

3.1. Cohort characteristics

A flow chart of the sampled patients was shown in Fig. 1. Of 248 consecutive patients who underwent initial CAS and had received preoperative cervical CTA at our institution, 67 patients were excluded because of nonatherosclerotic etiology of carotid artery stenosis (n = 15), acute infectious diseases (n = 7), and poor or partly absent image quality (n = 45). Finally, 181 patients, including 43 ISR cases and 138 non-ISR cases were enrolled. Of the 43 patients, 1 symptomatic underwent simple balloon dilatation and 2 symptomatic was treated with carotid endarterectomy. The other 40 asymptomatic patients were subjected to a standardized treatment regimen and close follow-up observation. The baseline clinical and demographic characteristics between the groups are presented in Table 1.

3.2. Comparison of variables between the ISR and non-ISR groups

Compared with the non-ISR group, patients with ISR showed a higher proportion of closed-cell stents (48.8% versus 27.5%; $p = 0.009$), greater degree of residual stenosis (28 [20,33] % versus 20 [14.75,30] %; $p < 0.001$). Additionally, the ISR group had a higher mean HU of PFD than the non-ISR group on the operated side (−42.26 ± 6.81 versus −59.66 ± 10.75; $p < 0.001$). For the contralateral side, no significant difference was observed in the mean HU of PFD between the two groups ($p > 0.05$). No significant difference was observed between the ISR groups and non-ISR groups ($p > 0.05$, Table 1), regarding the mean age of patients, the number of males, rates of hypertension, diabetes mellitus, hyperlipidemia, coronary heart disease, predilation, and postdilation.

Univariate logistic regression demonstrated a significant association between ISR and the degree of residual stenosis, the frequency of closed-cell stents used, and the mean HU of PFD on the operated side. Multivariate logistic regression showed that the degree of residual stenosis (OR 1.146, 95%CI 1.071–1.226, $P < 0.001$) and the mean HU of PFD on the operated side (OR1.353, 95%CI 1.215–1.506, $p < 0.001$) were significantly associated with ISR (Table 2).

3.3. The ROC curves of PFD for predicting ISR

In the analysis of ROC curves, the best cutoff value for predicting the occurrence of ISR was −53.85 HU, which has a sensitivity of

Table 1
Demographic and clinical characteristics of study patients.

Variable	All Patients (n = 181)	In-Stent Restenosis (n = 43)	No In-Stent Restenosis (n = 138)	*p* Value
Age, year	63.85 ± 7.48	64.67 ± 7.27	63.09 ± 7.64	0.157
Gender, male	137 (75.7)	32 (74.4)	105 (76.1)	0.824
BMI, kg/m^2	24.31 ± 2.37	24.74 ± 2.58	24.99 ± 2.61	0.590
Hypertension	108 (59.6)	29 (67.4)	79 (57.2)	0.234
Diabetes mellitus	80 (44.2)	24 (55.8)	56 (40.6)	0.079
Dyslipidemia	52 (28.7)	16 (37.2)	36 (26.1)	0.159
Current smoking	79 (43.6)	20 (46.5)	59 (42.8)	0.664
Coronary artery disease	17 (0.09)	2 (4.7)	15 (10.9)	0.222
Predilation	64 (35.3)	17 (39.5)	47 (34.1)	0.512
Postdilation	56 (30.9)	14 (32.6)	42 (30.4)	0.793
Degree of residual stenosis (%)	22 (15.5,30)	28 (20,33)	20 (14.75,30)	<0.001
Closed-cell stent	59 (32.6)	21 (48.8)	38 (27.5)	0.009
Mean HU of PFD (operated side)	−55.53 ± 12.40	−42.26 ± 6.81	−59.66 ± 10.75	<0.001
Mean HU of PFD (contralateral side)	−62.98 ± 10.72	−64.62 ± 8.42	−62.48 ± 11.32	0.252

The values are presented as the mean ± SD or median (P25 and P75) for continuous variables and as a number (percentages) for categorical variables.
Abbreviations: BMI, body mass index; Mean HU, Mean Hounsfield Units; PFD, perivascular fat density.

Table 2
Univariate analysis and a multivariate model for predicting carotid in-stent restenosis.

Variable	Univariate analysis		Multivariate analysis	
	OR (95% CI)	*p* value	OR (95% CI)	*p* value
Age, year	1.014 (0.968–1.062)	0.565		
Gender, male	0.914 (0.415–2.012)	0.824		
BMI, kg/m^2	0.964 (0.843–1.102)	0.588		
Hypertension	1.547 (0.752–3.183)	0.236		
Diabetes mellitus	1.850 (0.927–3.692)	0.081		
Hyperlipidemia	1.679 (0.813–3.469)	0.162		
Current smoking	1.164 (0.585–2.316)	0.665		
Coronary artery disease	0.400 (0.088–1.824)	0.237		
Predilation	1.266 (0.625–2.563)	0.512		
Postdilation	1.103 (0.530–2.298)	0.793		
Degree of residual stenosis (%)	1.073 (1.032–1.116)	<0.001	1.146 (1.071–1.226)	<0.001
Closed-cell stent	2.512 (1.241–5.084)	0.010	1.544 (0.500–4.767)	0.450
Mean HU of PFD (operated side)	1.254 (1.165–1.350)	<0.001	1.353 (1.215–1.506)	<0.001
Mean HU of PFD (contralateral side)	0.982 (0.951–1.013)	0.252		

Abbreviations: CI, confidence interval; Mean HU, Mean Hounsfield Units; PFD, perivascular fat density.

97.67% and specificity of 69.57% (area under the curve: 0.912; 95% CI: 0.861–0.949; $P < 0.001$; Fig. 4).

3.4. Interclass correlation coefficients and the consistency of measuring devices for PFD

Intraobserver reliability was substantially high between the two radiologists with interclass correlation coefficients (ICC) of 0.983 (95CI% 0.978–0.988) and 0.972 (95CI% 0.959–0.980) for mean HU on the operated and contralateral side, respectively (Table 3). The largest disagreement between the 2 observers obtained on a single case was 12 HU. Comparative analysis among the three CT scanners for the mean HU of PFD by the Kruskall-Wallis test presented no significant difference ($P > 0.05$), thus reducing the possible bias associated with the type of equipment (Table S2).

4. Discussion

This observational study provided an objective assessment of the association between the carotid arteries PFD and early ISR after CAS. Results have shown that an increased PFD is associated with the presence of early ISR after CAS. PFD can be used as an imaging marker to evaluate local carotid inflammation and might be an independent predictor of postoperative ISR in CAS patients. These findings may provide novel insights into treatment and prevention strategies for disease complications at an early stage.

Various predictors of in-stent restenosis, such as advanced age [23], female sex [23,24], diabetes mellitus [24,25], hyperlipidemia [24,26], and smoking [25] after CAS, have been proposed by previous studies. Tokunaga et al. have revealed that high-intensity signal on time-of-flight magnetic resonance angiography is associated with an increased risk of ISR, and intraplaque hemorrhage is a

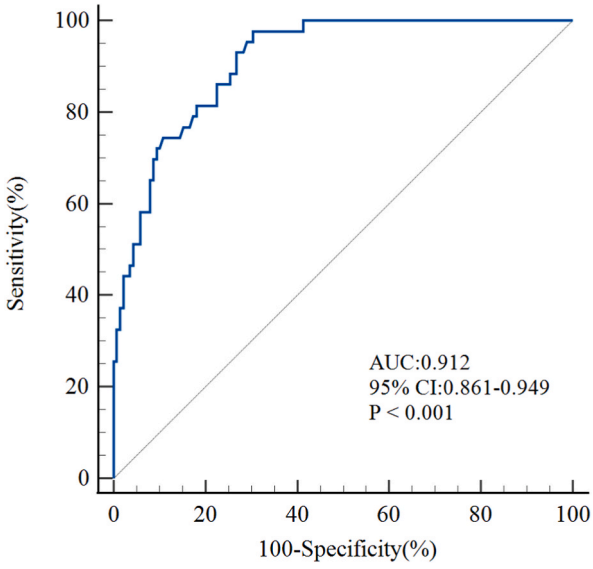

Fig. 4. The ROC curves of PFD were performed to predict ISR.

Table 3
The intraclass correlation coefficient for mean HU on computed tomographic angiography.

Variable	Intraclass Correlation	95% CI
Mean HU of PFD (operated side)	0.983	0.978–0.988
Mean HU of PFD (contralateral side)	0.972	0.959–0.980

Abbreviations: CI, confidence interval; Mean HU, Mean Hounsfield Units; PFD, perivascular fat density.

predictor of ISR after CAS [27]. Despite that few studies have addressed the association between PFD and in-stent restenosis after CAS, one study has histologically proven that PFD surrounding the carotid artery on CTA is associated with plaque vulnerability, which is characterized by fibrosis cap thinning and/or rupture and intraplaque hemorrhage. Speculations are made that PFD might be used as an indirect imaging marker for instability plaque [28,29]. The fast process and wide availability are the benefits of CTA, widely available as a noninvasive routine preoperative examination and used for detecting features of vulnerable plaques and assessing carotid artery inflammation [11,29]. A thorough search of the literature shows this study is the first to show that the PFD surrounding the responsible carotid artery on preoperative CTA is significantly associated with early ISR after CAS.

Moreover, early ISR after CAS is attributed to neointimal hyperplasia and vascular remodeling as a response to mechanical injury from balloon angioplasty and the self-expanding stent [30,31]. Specifically, vascular smooth muscle cell proliferation and migration are the primary causes of neointimal hyperplasia following stent implantation [32]. Inflammatory responses play a critical role in this pathological process. Reactive oxygen species derived from the inflammatory response can activate vascular smooth muscle cells, and stimulate their proliferation and migration, resulting in the remodeling of early-stage myofibroblasts or smooth muscle cells located in the vascular medial region [33]. Additionally, A high PFD correlates closely with inflammation-related histopathological markers [34]. Based on our assumption, the mechanism of the positive association between increased PFD value and occurrence of in-stent restenosis after CAS is neointimal hyperplasia accelerated by local carotid inflammation after CAS.

Histopathologic studies have demonstrated a key role of inflammation in carotid atherosclerotic plaque destabilization [35]. Pericarotid adipose tissue is a metabolically and immunologically active fat deposit implicated in atherogenesis. PFD reflects local carotid inflammatory, components, and pathological characteristics of carotid artery atherosclerotic plaques and can be used to assess local inflammatory activity in carotid unstable plaques [29]. When stents are placed in a vulnerable plaque, PVAT promotes local oxidative stress and triggers “outside-in” pathological signaling in the vessel wall, leading to massive secretion of proinflammatory factors, vascular smooth muscle cell dysfunction, and neointimal hyperplasia [36,37]. From our assumption, this explains the significant association between early ISR and increased PFD in preoperative carotid CTA.

From multivariable analysis, we discovered the degree of residual stenosis significantly contributed to the development of early ISR. The findings of this study matched those of previous research [38,39]. Thus, a reduction of residual stenosis for adequate revascularization is vital for reducing the occurrence of ISR. Our results also suggest that rates of the used closed-cell stent are higher in patients with ISR, which agree with that of other studies [40,41]. A possible explanation for this result is that the stiffer and denser material structure of closed-cell stents may lead to greater irritation of the vessel wall and stimulate neointimal proliferation [40].

Some limitations to this study are as follows: First, it was a retrospective, single-center study, whose only sampled patients were those with ISR that occurred early (up to 2 years after the initial CAS). Subgroup analyses of ISR were not performed because of the limited number of patients. The selection bias was enrolled inevitably. The predictive effect of increased PFD as an imaging marker for ISR after CAS cannot be fully determined. Larger future prospective studies with adequate longer imaging follow-ups are required. Second, we used CTA images based on the NASCET criteria to measure the degree of restenosis during the follow-up period and to define ISR. Although CTA defines ISR more accurately compared with the conventional Doppler ultrasound criteria, which has in-stent flow velocities that may be affected by stent placement and different stent types [38]. Additionally, CTA is difficult to perform and requires routine long-term follow-up. Third, the PFD measurements could be affected by the placement of the ROI. To ensure uniform ROI placement, we placed two circular ROIs around the carotid artery as described in previous studies [11], even though these ROI sites might not be the most severely inflamed areas. Moreover, different CT scanners are used to measure the HU values, which may affect the homogeneity of values and limit our ability to compare these values between patients [42]. Future prospective studies with dedicated quantitative software for analyzing PFD are warranted. As a final note, there was uncertainty in the range of the PFD measurements; because we adopted a commonly used approach, which is commonly used in studies of coronary arteries [43].

5. Conclusion

The results highlight PFD as a potential novel imaging marker for the predictive detection of early ISR after CAS, which may enable early initiation of protective therapy and reduce the incidence of early ISR and other postoperative complications.

Author contribution statement

Jun Hu, Na Hu: Conceived and designed the experiments; Analyzed and interpreted the data; Contributed reagents, materials, analysis tools or data; Wrote the paper.

Tiemin Hu, Jiwei Zhang, Dong Han: Contributed reagents, materials, analysis tools or data; Wrote the paper.

Hong Wang: Conceived and designed the experiments; Wrote the paper.

Funding

The present study was funded by the Science and Technology Program of Chengde (Grant No. 202006A086).

Data availability statement

Data will be made available on request.

Additional information

Supplementary content related to this article has been published online at [URL].

Declaration of competing interest

The authors declare that they have no known competing financial interests or personal relationships that could have appeared to influence the work reported in this paper.

Appendix A. Supplementary data

Supplementary data to this article can be found online at https://doi.org/10.1016/j.heliyon.2023.e16220.

References

[1] W.J. Powers, A.A. Rabinstein, T. Ackerson, O.M. Adeoye, N.C. Bambakidis, K. Becker, J. Biller, M. Brown, B.M. Demaerschalk, B. Hoh, E.C. Jauch, C.S. Kidwell, T.M. Leslie-Mazwi, B. Ovbiagele, P.A. Scott, K.N. Sheth, A.M. Southerland, D.V. Summers, D.L. Tirschwell, On behalf of the American heart association stroke council, guidelines for the early management of patients with acute ischemic stroke: 2019 update to the 2018 guidelines for the early management of acute ischemic stroke: a guideline for Healthcare professionals from the American heart association/American stroke association, Stroke 50 (2019), https://doi.org/10.1161/STR.0000000000000211.

[2] A. Ji, P. Lv, Y. Dai, X. Bai, X. Tang, C. Fu, J. Lin, Associations between carotid intraplaque hemorrhage and new ipsilateral ischemic lesions after carotid artery stenting: a quantitative study with conventional multi-contrast MRI, Int. J. Cardiovasc. Imag. 35 (2019) 1047–1054, https://doi.org/10.1007/s10554-018-01521-5.

[3] P. Lv, A. Ji, R. Zhang, D. Guo, X. Tang, J. Lin, Circumferential degree of carotid calcification is associated with new ischemic brain lesions after carotid artery stenting, Quant. Imag. Med. Surg. 11 (2021) 2669–2676, https://doi.org/10.21037/qims-20-1244.

[4] L.H. Bonati, J. Gregson, J. Dobson, D.J.H. McCabe, P.J. Nederkoorn, H.B. van der Worp, G.J. de Borst, T. Richards, T. Cleveland, M.D. Müller, T. Wolff, S. T. Engelter, P.A. Lyrer, M.M. Brown, A. Algra, S.J. Bakke, N. Baldwin, J. Beard, C. Bladin, J.M. Bland, J. Boiten, M. Bosiers, A.W. Bradbury, D. Canovas, B. Chambers, A. Chamorro, J. Chataway, A. Clifton, R. Collins, L. Coward, A. Czlonkowska, S. Davis, L. DeJaegher, D. Doig, P. Dorman, J. Ederle, R. F. Featherstone, J.M. Ferro, P. Gaines, G. Gilling-Smith, M. Goertler, A. Gottsäter, W. Hacke, A. Halliday, G. Hamilton, J.M.H. Hendriks, M. Hill, L.J. Kapelle, M. Kaste, F. Kennedy, P. Konrad, L. Kool, P.J. Koudstaal, I. Malik, H. Markus, P. Martin, J.-L. Mas, C. McCollum, T. McGahan, A.J. McGuire, P. Michel, A. Molyneux, J. Moroney, A. Mosch, J. Moss, R. Naylor, A. Peeters, D. Roy, D. Schultz, D.M. Seriki, R.A. Shinton, P. Sidhu, J. Stewart, G. Subramanian, R. Sztajzel, P.G. Than, D. Thomas, E. Turner, J.S.P. van den Berg, G. Vanhooren, G. Venables, N. Wahlgren, S. Walker, C. Warlow, B. Zvan, Restenosis and risk of stroke after stenting or endarterectomy for symptomatic carotid stenosis in the International Carotid Stenting Study (ICSS): secondary analysis of a randomised trial, Lancet Neurol. 17 (2018) 587–596, https://doi.org/10.1016/S1474-4422(18)30195-9.

[5] Z. Dai, G. Xu, Restenosis after carotid artery stenting, Vascular 25 (2017) 576–586, https://doi.org/10.1177/1708538117706273.

[6] C. Chaabane, F. Otsuka, R. Virmani, M.-L. Bochaton-Piallat, Biological responses in stented arteries, Cardiovasc. Res. 99 (2013) 353–363, https://doi.org/10.1093/cvr/cvt115.

[7] Z. Dai, R. Li, N. Zhao, Y. Han, M. Wang, S. Zhang, Y. Bai, Z. Li, M. Liang, L. Xiao, M. Ma, X. Liu, G. Xu, Neutrophil to lymphocyte ratio as a predictor of restenosis after angioplasty and stenting for asymptomatic carotid stenosis, Angiology 70 (2019) 160–165, https://doi.org/10.1177/0003319718784805.

[8] H. Shen, Z. Dai, M. Wang, S. Gu, W. Xu, G. Xu, X. Liu, Preprocedural neutrophil to albumin ratio predicts in-stent restenosis following carotid angioplasty and stenting, J. Stroke Cerebrovasc. Dis. 28 (2019) 2442–2447, https://doi.org/10.1016/j.jstrokecerebrovasdis.2019.06.027.

[9] M. Margaritis, F. Sanna, G. Lazaros, I. Akoumianakis, S. Patel, A.S. Antonopoulos, C. Duke, L. Herdman, C. Psarros, E.K. Oikonomou, C. Shirodaria, M. Petrou, R. Sayeed, G. Krasopoulos, R. Lee, D. Tousoulis, K.M. Channon, C. Antoniades, Predictive value of telomere length on outcome following acute myocardial infarction: evidence for contrasting effects of vascular vs. blood oxidative stress, Eur. Heart J. 38 (2017) 3094–3104, https://doi.org/10.1093/eurheartj/ehx177.

[10] C. Antoniades, A.S. Antonopoulos, J. Deanfield, Imaging residual inflammatory cardiovascular risk, Eur. Heart J. (2019), ehz474, https://doi.org/10.1093/eurheartj/ehz474.

[11] H. Baradaran, P.K. Myneni, P. Patel, G. Askin, G. Gialdini, K. Al-Dasuqi, H. Kamel, A. Gupta, Association between carotid artery perivascular fat density and cerebrovascular ischemic events, J. Am. Heart Assoc. 7 (2018), e010383, https://doi.org/10.1161/JAHA.118.010383.

[12] Xiaohong Hu, Jianhui Chen, Huajun Fu, Yinjuan Chen, Daofeng Fan, Yangui Chen, Chaoxiong Shen, Association between carotid artery perivascular fat density and embolic stroke of undetermined source, Front. Neurol. 12 (2022), 765962, https://doi.org/10.3389/fneur.2021.765962.

[13] Shuai Zhang, Hui Gu, Xinxin Yu, Bing Kang, Xianshun Yuan, Ximing Wang, Association between carotid artery perivascular fat density and intraplaque hemorrhage, Front. Cardiovasc. Med. 8 (2021), 735794, https://doi.org/10.3389/fcvm.2021.735794.

[14] L.H. Bonati, S. Kakkos, J. Berkefeld, G.J. de Borst, R. Bulbulia, A. Halliday, I. van Herzeele, I. Koncar, D.J. McCabe, A. Lal, J.-B. Ricco, P. Ringleb, M. Taylor-Rowan, H.-H. Eckstein, European Stroke Organisation guideline on endarterectomy and stenting for carotid artery stenosis, Eur. Stroke J. 6 (2021), https://doi.org/10.1177/23969873211012121. I–XLVII.

[15] N. Ar, R. Jb, B. Gj de, S. D, H.J. de, A. H, G. H, J. K, S. K, S. L, M. Hs, Dj M, J. R, H. S, van den B. Jc, F. V, E.G.C. None, P. K, N. C, Rj H, I. K, L. Js, V. de C M, V.F.E. G.R. None, B.S. A J, K.M. C A, P.F. L Ak, M. V, Editor's choice - management of atherosclerotic carotid and vertebral artery disease: 2017 clinical practice guidelines of the European society for vascular surgery (ESVS), Eur. J. Vasc. Endovasc. Surg. Off. J. Eur. Soc. Vasc. Surg. 55 (2018), https://doi.org/10.1016/j.ejvs.2017.06.021.

[16] S. Zhang, X. Yu, H. Gu, B. Kang, N. Guo, X. Wang, Identification of high-risk carotid plaque by using carotid perivascular fat density on computed tomography angiography, Eur. J. Radiol. 150 (2022), 110269, https://doi.org/10.1016/j.ejrad.2022.110269.

[17] V. Trisal, T. Paulson, S.S. Hans, V. Mittal, Carotid artery restenosis: an ongoing disease process, Am. Surg. 68 (2002) 275–279, discussion 279-280.

[18] K. Zhou, Y. Cao, X.-H. He, Z.-M. Qiu, S. Liu, Z.-L. Gong, J. Shuai, Q.-W. Yang, A comparison of safety and effectiveness between wingspan and neuroform stents in patients with middle cerebral artery stenosis, Front. Neurol. 12 (2021), 527541, https://doi.org/10.3389/fneur.2021.527541.

[19] Dan-Hong Zhang, Jiao-Lei Jin, Cheng-Fei Zhu, Qiu-Yue Chen, Xin-Wei He, Association between carotid artery perivascular fat density and cerebral small vessel disease, Aging 13 (2021) 18839–18851, https://doi.org/10.18632/aging.203327.

[20] Y. Miura, H. Kanamaru, R. Yasuda, N. Toma, H. Suzuki, Nonfasting triglyceride as an independent predictor of carotid restenosis after carotid endarterectomy or carotid artery stenting, World Neurosurg 156 (2021) e415–e425, https://doi.org/10.1016/j.wneu.2021.09.091.

[21] R. Niculescu, E. Russu, E.M. Arbănași, R. Kaller, E.M. Arbănași, R.M. Melinte, C.M. Coșarcă, I.G. Cocuz, A.H. Sabău, A.C. Tinca, A. Stoian, V. Vunvulea, A. V. Mureșan, O.S. Cotoi, Carotid plaque features and inflammatory biomarkers as predictors of restenosis and mortality following carotid endarterectomy, Int. J. Environ. Res. Publ. Health 19 (2022), 13934, https://doi.org/10.3390/ijerph192113934.

[22] M. Kuwabara, S. Sakamoto, T. Okazaki, D. Ishii, M. Hosogai, Y. Maeda, N. Horie, Factors contributing to restenosis after carotid artery stenting and the usefulness of magnetic resonance plaque imaging: a study of 308 consecutive patients, Eur. J. Radiol. 154 (2022), 110398, https://doi.org/10.1016/j.ejrad.2022.110398.

[23] M.A. Khan, M.W. Liu, F.L. Chio, G.S. Roubin, S.S. Iyer, J.J. Vitek, Predictors of restenosis after successfulcarotid artery stenting, Am. J. Cardiol. 92 (2003) 895–897, https://doi.org/10.1016/S0002-9149(03)00912-3.

[24] B.K. Lal, K.W. Beach, G.S. Roubin, H.L. Lutsep, W.S. Moore, M.B. Malas, D. Chiu, N.R. Gonzales, J.L. Burke, M. Rinaldi, J.R. Elmore, F.A. Weaver, C.R. Narins, M. Foster, K.J. Hodgson, A.D. Shepard, J.F. Meschia, R.O. Bergelin, J.H. Voeks, G. Howard, T.G. Brott, CREST Investigators, Restenosis after carotid artery stenting and endarterectomy: a secondary analysis of CREST, a randomised controlled trial, Lancet Neurol. 11 (2012) 755–763, https://doi.org/10.1016/S1474-4422(12)70159-X.

[25] S. Ronchey, B. Praquin, M. Orrico, E. Serrao, C. Ciceroni, V. Alberti, S. Fazzini, N. Mangialardi, Outcomes of 1000 carotid wallstent implantations: single-center experience, J. Endovasc. Ther. 23 (2016) 267–274, https://doi.org/10.1177/1526602815626558.

[26] R. Topakian, M. Sonnberger, K. Nussbaumer, H.-P. Haring, J. Trenkler, F.T. Aichner, Postprocedural high-density lipoprotein cholesterol predicts carotid stent patency at 1 year: HDL cholesterol and carotid stent patency, Eur. J. Neurol. 15 (2008) 179–184, https://doi.org/10.1111/j.1468-1331.2007.02026.x.

[27] K. Tokunaga, S. Tokunaga, K. Hara, M. Yasaka, Y. Okada, T. Kitazono, T. Tsumoto, Intraplaque high-intensity signal on time-of-flight magnetic resonance angiography and restenosis after carotid artery stenting, J. Neurosurg. 136 (2022) 1029–1034, https://doi.org/10.3171/2021.4.JNS21546.

[28] M. Yu, Y. Meng, H. Zhang, W. Wang, S. Qiu, B. Wang, Y. Bao, B. Du, S. Zhu, Y. Ge, L. Zhu, K. Xu, Associations between pericarotid fat density and image-based risk characteristics of carotid plaque, Eur. J. Radiol. 153 (2022), 110364, https://doi.org/10.1016/j.ejrad.2022.110364.

[29] L. Saba, S. Zucca, A. Gupta, G. Micheletti, J.S. Suri, A. Balestrieri, M. Porcu, P. Crivelli, G. Lanzino, Y. Qi, V. Nardi, G. Faa, R. Montisci, Perivascular fat density and contrast plaque enhancement: does a correlation exist? AJNR Am. J. Neuroradiol. 41 (2020) 1460–1465, https://doi.org/10.3174/ajnr.A6710.

[30] E.J. Armstrong, D.G. Kokkinidis, Restenosis after carotid artery stenting, Cardiovasc. Revascularization Med. 24 (2021) 70–71, https://doi.org/10.1016/j.carrev.2021.01.007.

[31] S.A. Goel, L.-W. Guo, B. Liu, K.C. Kent, Mechanisms of post-intervention arterial remodelling, Cardiovasc. Res. 96 (2012) 363–371, https://doi.org/10.1093/cvr/cvs276.

[32] A. Farb, D.K. Weber, F.D. Kolodgie, A.P. Burke, R. Virmani, Morphological predictors of restenosis after coronary stenting in humans, Circulation 105 (2002) 2974–2980, https://doi.org/10.1161/01.CIR.0000019071.72887.BD.

[33] K.K. Griendling, G.A. FitzGerald, Oxidative stress and cardiovascular injury: Part II: animal and human studies, Circulation 108 (2003) 2034–2040, https://doi.org/10.1161/01.CIR.0000093661.90582.c4.

[34] A.S. Antonopoulos, F. Sanna, N. Sabharwal, S. Thomas, E.K. Oikonomou, L. Herdman, M. Margaritis, C. Shirodaria, A.-M. Kampoli, I. Akoumianakis, M. Petrou, R. Sayeed, G. Krasopoulos, C. Psarros, P. Ciccone, C.M. Brophy, J. Digby, A. Kelion, R. Uberoi, S. Anthony, N. Alexopoulos, D. Tousoulis, S. Achenbach, S. Neubauer, K.M. Channon, C. Antoniades, Detecting human coronary inflammation by imaging perivascular fat, Sci. Transl. Med. 9 (2017), eaal2658, https://doi.org/10.1126/scitranslmed.aal2658.

[35] M. Marnane, S. Prendeville, C. McDonnell, I. Noone, M. Barry, M. Crowe, N. Mulligan, P.J. Kelly, Plaque inflammation and unstable morphology are associated with early stroke recurrence in symptomatic carotid stenosis, Stroke 45 (2014) 801–806, https://doi.org/10.1161/STROKEAHA.113.003657.

[36] F. Han, Y. Zhang, M. Shao, Q. Mu, X. Jiao, N. Hou, X. Sun, C1q/TNF-related protein 9 improves the anti-contractile effects of perivascular adipose tissue via the AMPK-eNOS pathway in diet-induced obese mice, Clin. Exp. Pharmacol. Physiol. 45 (2018) 50–57, https://doi.org/10.1111/1440-1681.12851.

[37] H. Hu, M. Garcia-Barrio, Z. Jiang, Y.E. Chen, L. Chang, Roles of perivascular adipose tissue in hypertension and atherosclerosis, antioxid, Redox Signal 34 (2021) 736–749, https://doi.org/10.1089/ars.2020.8103.

[38] A. Ösken, E. Akdeniz, M. Keskin, A. Öz, G. Ipek, R. Zehir, H. Barutça, N. Çam, S. Şahin, Estimated glomerular filtration rate as a predictor of restenosis after carotid stenting using first-generation stents, Angiology 72 (2021) 762–769, https://doi.org/10.1177/00033197211014684.

[39] K. Yamashita, J. Kokuzawa, T. Kuroda, S. Murase, M. Kumagai, Y. Kaku, In-stent hypodense area at two weeks following carotid artery stenting predicts neointimal hyperplasia after two years, NeuroRadiol. J. 31 (2018) 280–287, https://doi.org/10.1177/1971400917727006.

[40] M.D. Müller, J. Gregson, D.J.H. McCabe, P.J. Nederkoorn, H.B. van der Worp, G.J. de Borst, T. Cleveland, T. Wolff, S.T. Engelter, P.A. Lyrer, M.M. Brown, L. H. Bonati, For the international carotid stenting study investigators, stent design, restenosis and recurrent stroke after carotid artery stenting in the international carotid stenting study, Stroke 50 (2019) 3013–3020, https://doi.org/10.1161/STROKEAHA.118.024076.

[41] P. Texakalidis, S. Giannopoulos, D.G. Kokkinidis, G. Lanzino, Effect of open- vs closed-cell stent design on periprocedural outcomes and restenosis after carotid artery stenting: a systematic review and comprehensive meta-analysis, J. Endovasc. Ther. 25 (2018) 523–533, https://doi.org/10.1177/1526602818783505.

[42] B.A. Birnbaum, N. Hindman, J. Lee, J.S. Babb, Multi–detector row CT attenuation measurements: assessment of intra- and interscanner variability with an anthropomorphic body CT phantom, Radiology 242 (2007) 109–119, https://doi.org/10.1148/radiol.2421052066.

[43] E.K. Oikonomou, M. Marwan, M.Y. Desai, J. Mancio, A. Alashi, E. Hutt Centeno, S. Thomas, L. Herdman, C.P. Kotanidis, K.E. Thomas, B.P. Griffin, S.D. Flamm, A.S. Antonopoulos, C. Shirodaria, N. Sabharwal, J. Deanfield, S. Neubauer, J.C. Hopewell, K.M. Channon, S. Achenbach, C. Antoniades, Non-invasive detection of coronary inflammation using computed tomography and prediction of residual cardiovascular risk (the CRISP CT study): a post-hoc analysis of prospective outcome data, Lancet 392 (2018) 929–939, https://doi.org/10.1016/S0140-6736(18)31114-0.